Geophysical Research Letters

RESEARCH LETTER
10.1029/2019GL083249

Shock Vaporization/Devolatilization of Evaporitic Minerals, Halite and Gypsum, in an Open System Investigated by a Two-Stage Light Gas Gun

Kosuke Kurosawa[1], Ryota Moriwaki[1], Goro Komatsu[1,2], Takaya Okamoto[3], Hiroshi Sakuma[4], Hikaru Yabuta[5], and Takafumi Matsui[1]

[1]Planetary Exploration Research Center, Chiba Institute of Technology, Narashino, Japan, [2]International Research School of Planetary Sciences, Università d'Annunzio, Pescara, Italy, [3]Institute of Space and Astronautical Science, Japan Aerospace Exploration Agency, Sagamihara, Japan, [4]Research Center for Functional Materials, National Institute for Materials Science, Tsukuba, Japan, [5]Department of Earth and Planetary Systems Science, Graduate School of Science, Hiroshima University, Higashi–Hiroshima, Japan

Abstract Dry lakebeds might constitute large volatile reservoirs on Mars. Hypervelocity impacts onto ancient dry lakebeds would have affected the volatile distribution on Mars. We developed a new experimental method to investigate the response of evaporitic minerals (halite and gypsum) to impact shocks in an open system. This technique does not result in chemical contamination from the operation of the gas gun. The technique is termed the "two-valve method," and the gun system is located in the Planetary Exploration Research Center, Chiba Institute of Technology, Japan. We detected the vaporization of halite at 31 GPa and devolatilization from gypsum at 11 GPa, suggesting that impact-induced volatile release from dry lakebeds has periodically occurred throughout Martian history. The vaporization of halite deposits might have enhanced the production of perchlorates, which are found globally on Mars. The water loss from gypsum possibly explains the coexisting types of Ca-sulfates found in Gale Crater.

Plain Language Summary We used a new experimental technique to investigate the result of a meteoroid impact into an evaporitic deposit on Mars. Although two-stage light gas guns are ideal projectile launchers, the dirty gas from the gun has been a long-standing limitation of this technique that so far greatly complicated analysis of the vapors that are generated due to such impacts. Our new method overcomes this limitation and allows us to measure impact-generated vapor from evaporitic minerals. We detected NaCl vapor from halite and water vapor from gypsum at velocities lower than the typical impact velocities onto Mars. This suggests that volatile release from ancient dry lakebeds has periodically occurred throughout Martian history, due to stochastic meteoroid impacts. The nature of perchlorates and Ca-sulfates found on Mars can be interpreted as the result of hypervelocity impacts onto dry lakebeds rich in evaporitic minerals.

Key Points:
- Gas release from halite and gypsum was studied using a two-stage light gas gun setup that avoids contamination of impact vapors from gun-related gases
- Vaporization of halite at 31 GPa and devolatilization (water loss) from gypsum at 11 GPa were detected
- Impacts might have resulted in efficient production of perchlorates in Martian soil and produced the anhydrite found in Gale Crater

Supporting Information:
- Supporting Information S1

Correspondence to:
K. Kurosawa,
kosuke.kurosawa@perc.it-chiba.ac.jp

Citation:
Kurosawa, K., Moriwaki, R., Komatsu, G., Okamoto, T., Sakuma, H., Yabuta, H., & Matsui, T. (2019). Shock vaporization/devolatilization of evaporitic minerals, halite and gypsum, in an open system investigated by a two-stage light gas gun. *Geophysical Research Letters*, *46*, 7258–7267. https://doi.org/10.1029/2019GL083249

Received 9 APR 2019
Accepted 9 JUN 2019
Accepted article online 14 JUN 2019
Published online 3 JUL 2019

1. Introduction

The presence of evaporitic minerals, such as halite (NaCl) and gypsum ($CaSO_4 \cdot 2H_2O$), on a planet can be interpreted as evidence that wet conditions existed in the planet's geological history. For example, sedimentation of evaporites is an inevitable outcome when a lake evaporates under playa-like conditions (e.g., Komatsu et al., 2007). Minerals interpreted to be of evaporitic origin (i.e., sulfates and chlorides) have been found on Mars (e.g., Davila et al., 2011; McLennan et al., 2005; Osterloo et al., 2008). Here we consider the situation when hypervelocity impacts occur into ancient dry lakebeds rich in evaporitic minerals. Indeed, there appear to be impact craters in chloride-bearing deposits on Mars (Osterloo et al., 2010). The results of an impact into an evaporitic deposit have a number of interesting and diverse implications, including the promotion of perchlorate (ClO_4^-) formation and transformation of gypsum into anhydrite.

Recently, enrichment of chlorine (Cl) in the Martian surface with respect to bulk Mars has been detected, based on both the composition of Martian meteorites and remote sensing observations by a gamma ray spectrometer onboard the Mars Odyssey (e.g., Keller et al., 2006; Lodders & Fegley, 1997; Rao et al., 2002). The Phoenix lander and Curiosity rover have detected perchlorate (ClO_4^-) in Martian soil at high and low latitudes, respectively, which is one of the expressions of this excess Cl (e.g., Hecht et al., 2009; Kounaves

et al., 2014). This implies that perchlorates are widespread over the entire surface of Mars (Clark & Kounaves, 2016). Given that perchlorate is a powerful oxidant in the surface environment, the distribution and behavior of Cl are important in understanding the survivability of organics on Mars. If chlorine-bearing minerals coexist with silicate minerals, perchlorates can be efficiently produced via oxidative photochemistry by ultraviolet radiation (<280 nm; UV-C; Carrier & Kounaves, 2015) and galactic cosmic rays (Wilson et al., 2016), and via high-temperature plasma chemistry by electrical discharges in dust storms (Wu et al., 2018). Recently, a model combining these two potential scenarios has also been proposed (Martínez-Pabello et al., 2019). The remaining question is how a sufficient amount of chlorine-bearing minerals was supplied to Martian soil, which initially contained a similar amount of Cl as bulk Mars. If shock-induced vaporization of halite commonly occurs during impact events, then hypervelocity impacts might have promoted extensive lateral transport of Cl-bearing minerals from halite deposits to surrounding Martian soils.

In this study, we also focus on shock-induced devolatilization of gypsum. Although known large-scale gypsum deposits on Mars are limited to the gypsum dunes of Olympia Undae near the North Pole region (Ehlmann & Edwards, 2014; Fishbaugh et al., 2007), the CheMin X-ray diffraction instrument onboard Curiosity found the dehydrated forms of Ca-sulfates, basanite ($CaSO_4 \cdot 0.5H_2O$) and anhydrite ($CaSO_4$), as well as gypsum, in Gale Crater (e.g., Brake et al., 2013; Vaniman et al., 2018). The limited global-scale gypsum deposits and nonequilibrium nature of the sulfates in Gale Crater suggest that shock-induced water loss from gypsum has been an important geological process on Mars. In addition, shock-induced water loss from gypsum has been proposed as a new shock indicator (e.g., Bell & Zolensky, 2011).

To obtain insights into such processes, impact experiments on evaporite targets are desirable. For instance, the vaporization/devolatilization thresholds of evaporites are important to understand the thermodynamic response of evaporitic minerals to impacts. Two-stage light gas guns have been used to investigate impact-driven processes, because they can accelerate a macroscopic projectile (>0.1 mm in diameter) at room temperature up to velocities of several km/s (e.g., Kurosawa et al., 2012). To avoid chemical contamination from the gases used for the operation of these guns, most previous studies have been conducted in closed systems (e.g., Boslough et al., 1982; Furukawa et al., 2008; Martins et al., 2013), in which samples are completely covered by containers. In contrast, all natural impacts occur in open systems. The thermodynamic path during decompression from a shocked to reference state in a closed system is significantly different from that in an open system because (1) fast cooling of the shocked materials due to adiabatic expansion is prevented due to the limited volume of the container (e.g., Ivanov & Deutsch, 2002; Kurosawa et al., 2012) and (2) the total pressure in the closed system is supported by the mechanical strength of the container. Given that the mechanical strength of a container made of stainless steel reaches ~1 GPa (e.g., Nakazawa et al., 2005), the phase changes and chemical reactions proceed under high-pressure and low-temperature conditions (i.e., a low-entropy state) in a closed system. This situation is markedly different from natural impacts. Thus, impact experiments in an open system are essential to accurately understand impact-driven phenomena.

In a previous study, we developed an experimental technique using two-stage light gas guns (Kurosawa et al., 2012). This method allows us to conduct mass spectrometric analysis of gases generated in an open system using light gas guns. The method can prevent chemical contamination from the gun (Ishibashi et al., 2017; Kurosawa et al., 2012). However, the procedure requires use of a plastic diaphragm, which leads to destruction of weak projectiles, such as fused quartz (Kurosawa et al., 2012), and chemical contamination by trace amounts of carbon (ppm levels) due to carbon-bearing vapor produced by the penetration of the plastic diaphragm. This limitation prevents further applications of this method, such as accurate detection of incipient vaporization/devolatilization and a detailed investigation of complex organic species in impact-generated vapor. Thus, the objective of this study was to develop a system to investigate shock vaporization/devolatilization in an open system using a two-stage light gas gun without a diaphragm.

2. Experiments

We describe the detail of the experimental system developed in this study and experimental condition in section 2.1. The experimental procedure are described in section 2.2.

2.1. Experimental System and Condition

We used the gun system developed at the Planetary Exploration Research Center of Chiba Institute of Technology (PERC/Chitech), Japan (Kurosawa et al., 2015), which has two new automatic gate valves installed in the gun system. Figure 1a shows a schematic diagram of the system.

Natural samples of halite and gypsum were used as targets, which were shaped as blocks. The masses of the halite and gypsum blocks were ~1 and ~0.6 kg, respectively. The halite targets are polycrystalline aggregates of randomly oriented crystals. We used a polycrystalline form of gypsum that is referred to as satin spar gypsum. The gypsum was cut into several blocks, and all impacts were performed parallel to the *c* axis. Given the axial compressibility of gypsum is almost isotropic up to 4 GPa (Comodi et al., 2008), the effects of crystal orientation on shock-induced devolatilization are likely to be insignificant. The chemical and mineralogical compositions of the samples are summarized in Text S1 in the supporting information. We also used a natural basalt block as a target in a control experiment. Spheres made of oxides (i.e., fused quartz and Al_2O_3) were used as projectiles. The projectile diameters were set to 2.0 and 1.5 mm for the halite and gypsum, respectively. We used the smaller projectile in the experiments using gypsum targets because the sizes of the gypsum blocks were smaller than those of the halite blocks. A nylon-slit sabot (Kawai et al., 2010) was used to accelerate the projectiles. The impact velocity was varied from 1.9 to 7.2 km/s. The peak pressures at the impact point were estimated to be 10–110 GPa by the one-dimensional impedance method (e.g., Melosh, 1989). Hereafter, the peak pressure is referred to as the 1-D pressure $P_{1\text{-D}}$. The shock Hugoniot parameters were taken from previous studies (Ahrens & Johnson, 1995; Marsh, 1980; Melosh, 1989; Trunin et al., 2001), and the values actually used are summarized in Text S2. The experimental chamber was pressurized to an equilibrium pressure determined by the balance between He gas injection and the evacuation by the pump. This prevented the intrusion of the contaminant gases from the gun as described in section 2.2. The equilibrium pressure was set to 500 Pa. The target blocks were set on the target stage with a small tilt to minimize the damage to valve #2 by fast ejecta moving back in the direction of the projectile trajectory, which is frequently observed in cratering processes under the strength-dominated cratering regime (e.g., Hoerth et al., 2013). The impact angle was 80° from the target surface. Thus, the calculated $P_{1\text{-D}}$ values are slightly overestimated in this study.

2.2. Experimental Procedure

Prior to a shot, valves #1 and #2 are closed and opened, respectively. The gun side uprange from valve #1 is evacuated, and the green shaded region is filled with a chemically inert gas, such as helium (He). A gas flow is induced using a rotary pump. To maintain a constant ambient pressure in the experimental chamber, the inert gas is continuously introduced into the experimental chamber with the same gas flux as the evacuation. Using a pulse generator, signals with different time delays are inputted to valves #1 and #2 and the two-stage light gas gun. At the start, valve #1 is opened, leading to the expansion of inert gas into the dissipation chamber due to the strong pressure gradient. The gun is then operated, and a projectile is launched toward the target placed in the experimental chamber. The contaminant gas following the projectile is not able to intrude into the experimental chamber due to the outflow. In contrast, the solid projectile is able to penetrate into the outflow and impact the target. Since the time required for projectile acceleration is much shorter than the duration of the outflow, the impact occurs under a pressure that is ≥90% of the initial ambient pressure (see Text S3.1). Immediately after the impact, valve #2 is closed to keep the impact-generated vapor in the experimental chamber. Subsequently, the gas generated by the impact is introduced into a quadrupole mass spectrometer (Pfeiffer vacuum, Prisma plus QMG220) by the inert gas flow produced by the rotary pump. This experimental method is termed the "two-valve method." Figure 1b shows a time-stacked image of a fused quartz projectile immediately before the impact, clearly showing that the projectile was completely intact before the impact. Thus, the two-valve method allows us to use any combination of projectile and target.

To detect water vapor from gypsum, we used a cold trap placed at the bottom of the target stage to reduce the background water vapor in the chamber. We used liquid nitrogen (N_2) as a refrigerant. The temperature of the gypsum target prior to a shot was monitored with a thermocouple. The typical target temperature prior to a shot was ~250 K, which is intermediate between the average surface temperature (~210 K) and maximum diurnal temperature near the equator (~290 K) on Mars.

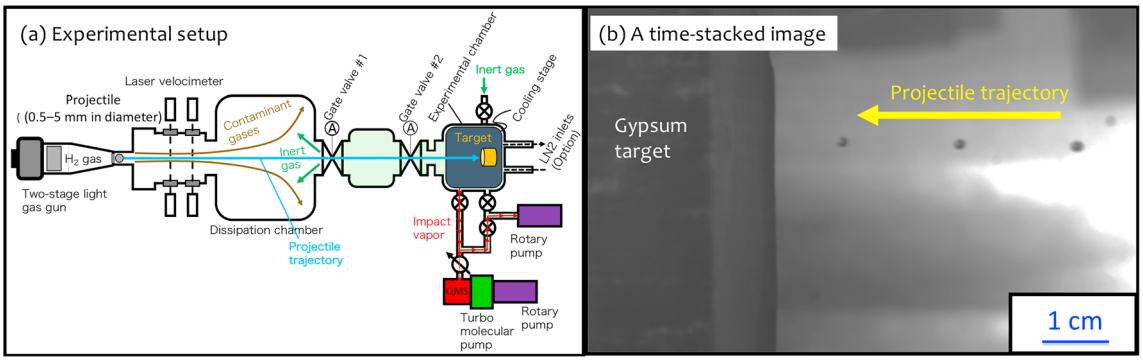

Figure 1. (a) Schematic diagram of the experimental system. (b) A time-stacked image of a flying projectile prior to an impact. The time interval between images is 4 μs.

3. Results

Experimental results on halite and gypsum are presented in sections 3.1 and 3.2, respectively, along with the mass spectrometry results on the shock-generated gases. The ion current for the mass number $M/Z = i$ is denoted as I_i. We also conducted another series of impact experiments using natural calcite samples to characterize the experimental system (Text S3). We confirmed that the intrusion of contaminant gas from the gun was reduced to ~1 μg, which corresponds to 0.01–0.1 wt.% of the projectile mass.

3.1. Shock Vaporization of Halite

Figure 2a shows a typical example of the temporal variations of the ion currents at selected mass numbers. We detected a sudden rise in I_{58} ($Na^{35}Cl^+$) and I_{70} ($^{35}Cl_2{}^+$) after the impact, although the peak current ratios I_{58}/I_4 and I_{70}/I_4 were only 0.1–1.0 ppm. Although we only show the ion currents of ^{35}Cl-bearing species, we observed similar trends for species containing ^{37}Cl, such as I_{60} ($Na^{37}Cl^+$), I_{71} ($^{36}Cl^{37}Cl^+$), and I_{72} ($^{37}Cl_2{}^+$). The I_i to I_4 (He^+) ratio approximates the partial pressure of species i in the experimental chamber, because the total pressure in the chamber was mostly supported by He (Text S3.3). We also detected a rise in I_{18} (H_2O^+), possibly from adsorbed water due to the highly hygroscopic nature of halite. The rise in I_2 ($H_2{}^+$) is likely to be caused by the cracking of H_2O by electron impacts in the quadrupole mass spectrometer. This rise was not due to the intrusion of contaminant gas from the gun, because the rise in I_2 in the experiments on natural calcite targets was much smaller than those in the halite experiments (see Text S3.2).

Figure 3a shows the temporal variations in I_{58}/I_4 at different shock pressures. We found that halite initiates vaporization between 18 and 31 GPa.

3.2. Shock-Induced Water Release From Gypsum

Figure 2b is the same as Figure 2a except that gypsum was the target. The cold trap allowed us to reduce the background level of I_{18} down to ~1/30, as compared with the case of the halite experiments (Figure 2a). Shock-generated water vapor was clearly detected. In contrast, sulfur-bearing gases, such as SO, SO_2, and SO_3, did not clearly increase after the impact even at 7.2 km/s. The estimated 1-D pressure of this shot reaches $P_{1\text{-D}} = 114$ GPa. Note that the time when I_{18} becomes the maximum was delayed up to ~50 s after the time at the impact.

Figure 3b shows the same as Figure 3a except that the target was gypsum and I_{18}/I_4 is shown. We observed increases in I_{18}/I_4 even at 2.0 km/s. In contrast, I_{18}/I_4 remained at the background level in the blank experiment, which used a basalt block at the same impact velocity of 2.0 km/s, suggesting that gypsum experienced water loss at $P_{1\text{-D}} < 11$ GPa. In the control experiment, a fused quartz projectile was accelerated to 2.0 km/s. Thus, we can rule out the possibility that the detected water vapor in the gypsum experiment at the lowest impact velocity (2.0 km/s) comes from the desorption of water vapor from the chamber wall/floor or the projectile.

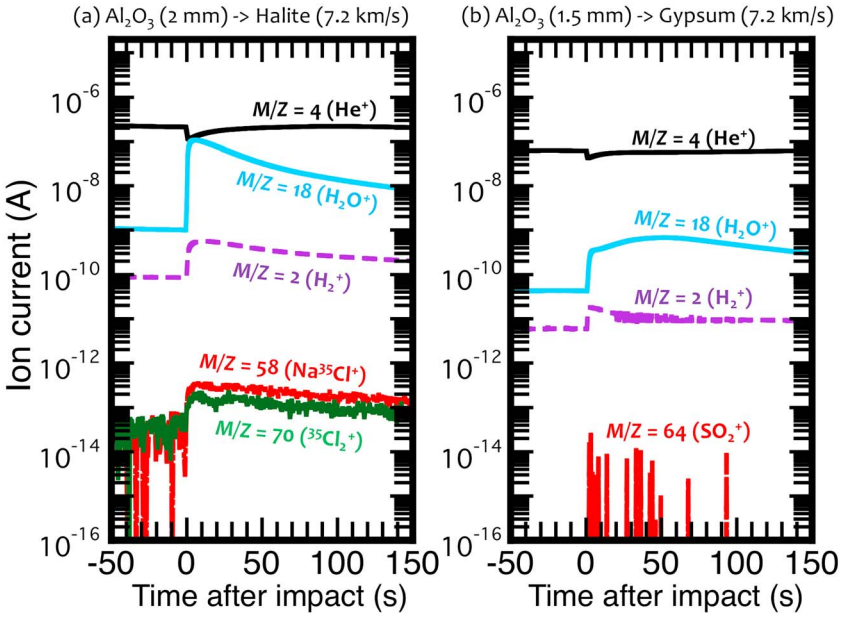

Figure 2. Time variations of the ion currents for the selected species for (a) halite and (b) gypsum. The projectile diameters and impact velocities of the shots are indicated on top of the figure.

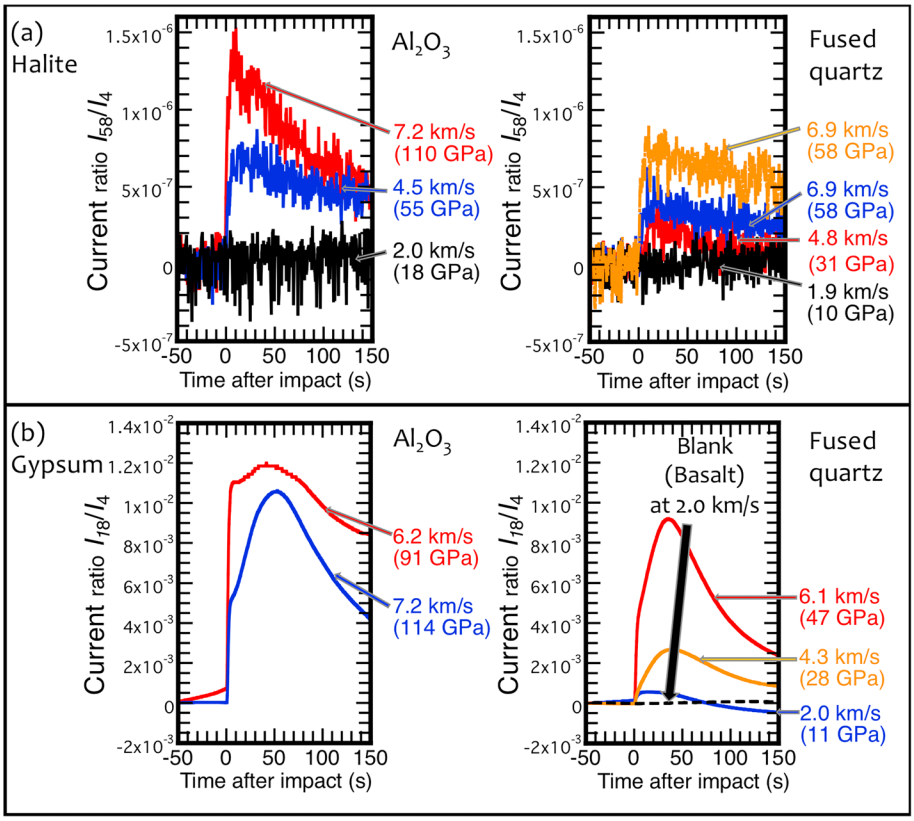

Figure 3. Time variations of the current ratios I_{58}/I_4 ($Na^{35}Cl^+/He^+$, a) and I_{18}/I_4 (H_2O^+/He^+, b). The results for the (a) halite and (b) gypsum targets are shown. The results for Al_2O_3 and quartz projectiles are displayed at the left and right panels, respectively. The rises in I_{58}/I_4 and I_{18}/I_4 corresponds to the generation of NaCl and water vapor, respectively.

4. Discussion

In our experimental system, accurate quantitative measurements of the gases produced are not available due to gas escape from the chamber through valve #2 prior to its closure (see Text S3.5). As such, we mainly discuss the initiation of evaporite vaporization/devolatilization with increasing 1-D pressure in section 4.1. The initiation can be determined by the presence or absence of sudden increases in the ion current ratios after the impacts. We then discuss the chemical composition of the vapor generated from gypsum in section 4.2. The implications of our results are discussed in section 4.3.

4.1. Vaporization/Devolatilization Threshold

We estimated the boiling point of pure NaCl to be ~1,200 K using a Gibbs energy minimization method (e.g., Gordon & McBride, 1994) at 500 Pa (see Text S4). We used 1,200 K as an approximate temperature required for incipient vaporization of halite because we confirmed that the halite targets are mainly composed of NaCl (99.5 wt.%; Text S1). According to a previous study (Ballirano & Melis, 2009), water release from gypsum in a vacuum occurs at ~370 K. If the postshock temperatures T_{post} after pressure release down to 500 Pa exceed the above temperatures (i.e., 1,200 K for halite and 370 K for gypsum), then vaporization/devolatilization should occur (e.g., Ahrens & O'Keefe, 1972; Ivanov & Deutsch, 2002; Kurosawa et al., 2012). The ambient pressure in the experimental chamber before the closure of valve #2 decreases to ~350 Pa, although we assumed the reference pressure to be 500 Pa. If we use the minimum ambient pressure (350 Pa) as the reference pressure, the boiling point of NaCl becomes 1,150 K. This does not affect the conclusions described below. Figure 4 shows the postshock temperature as a function of $P_{1\text{-}D}$. We calculated T_{post} in two steps as described as follows. First, we calculated the shock-induced entropy gain using the method proposed by Sugita et al. (2012). In this calculation, we used the shock Hugoniot parameters and Mie-Grüneisen equation of state and adopted the Dulong-Petit value for the constant isochoric specific heat. Second, we calculated the difference in temperature between the initial state and postshock state by assuming isentropic release from the peak shock state (e.g., Senshu et al., 2002). We found that vaporization/devolatilization from the evaporitic minerals occurs at systematically lower $P_{1\text{-}D}$ than expected from these simple thermodynamic estimates. This does not necessarily mean that the theoretical estimates are incorrect because of the reasons as follows. Although most previous experiments have reported the shock pressure required for incipient vaporization/devolatilization based on whether shock-generated gases were detected at a given shock pressure, our results suggest that local energy concentration due to the processes, such as jetting (e.g., Kieffer, 1977), shear banding (Kondo & Ahrens, 1983), and irreversible heating due to friction and plastic deformation (Kurosawa & Genda, 2018), largely contributes to the initiation of gas release with increasing $P_{1\text{-}D}$. Consequently, experimental assessment of the shock pressure required for initiating gas release are complicated by disequilibrium energy partitioning into local regions and/or strength-induced irreversible heating.

We now consider the differences in spatial scale between experimental and natural impact events. The spatial scale of natural impacts is at least several orders of magnitude greater than that of laboratory-scale impacts, leading to a much lower cooling/decompression rate in natural impact events. Given that we can assume thermodynamic equilibrium and no heat production during pressure release (i.e., an adiabatic process), the decompression path on a pressure–temperature plane should be the same for natural and laboratory-scale impacts (e.g., Ahrens & O'Keefe, 1972), although the times required for complete decompression are quite different (e.g., Ishimaru et al., 2010). In this case, the simple thermodynamic estimates based on T_{post} to determine the pressure required for incipient vaporization/devolatilization (i.e., water loss) can be applied to natural impacts.

The maximum degree of impact heating due to the local energy concentration caused by jetting and shear banding would not be strongly dependent on the spatial scale, because it is determined by the local flow/stress field during an impact (e.g., Kieffer, 1977; Kondo & Ahrens, 1983). However, heating due to plastic deformation in pressure-strengthened rocks during pressure release (Kurosawa & Genda, 2018) is potentially a scale-dependent process, although this has not been investigated. Melosh and Ivanov (2018) noted that the yield stress of rocky materials also depends on the strain rate, although Kurosawa and Genda (2018) used a scale-independent strength model constructed from static failure data (e.g., Lundborg, 1968). A comparative study of laboratory/numerical impact experiments and natural samples that have

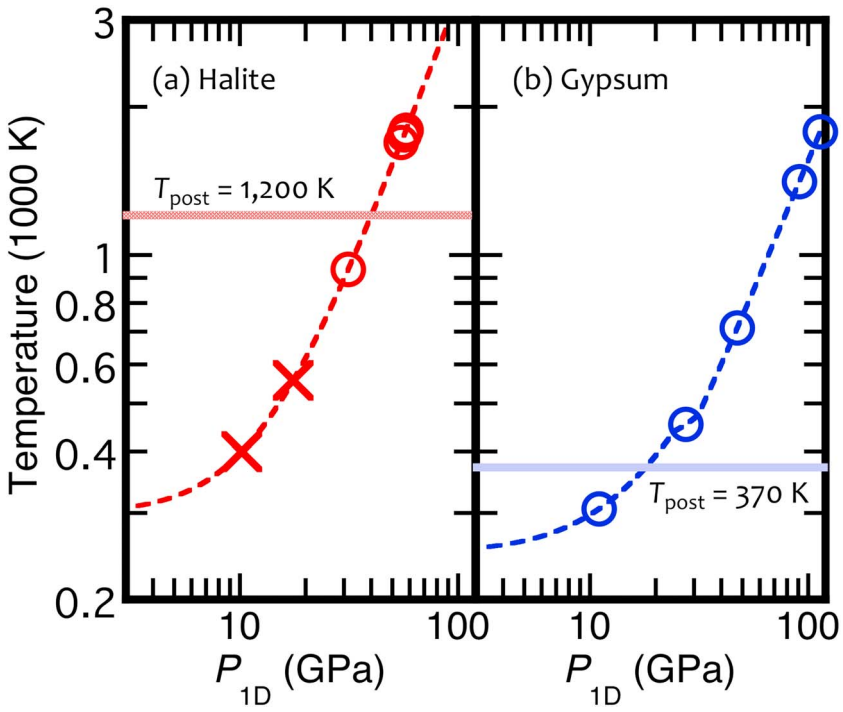

Figure 4. Post shock temperature for (a) halite and (b) gypsum as a function of the peak pressure at the impact point $P_{1\text{-}D}$. The data points on the curves indicate $P_{1\text{-}D}$ investigated in this study. The horizontal lines indicate the temperatures required for incipient vaporization and devolatilization (i.e., water loss; section 4.1). The circles indicate that the shock-generated gases were detected. The crosses represent that no gas release occurred.

experienced shock-induced metamorphism might provide a robust understanding of scaling effects on shock-induced vaporization/devolatilization. Such an investigation is the beyond the scope of the present study.

4.2. Stability of Sulfur During Impact Shocks

Release of sulfur-bearing gases from the gypsum targets was not clearly detected even at $P_{1\text{-}D}$ = 114 GPa (Figure 2b). Nevertheless, the required shock pressure for incipient/complete sulfur release from anhydrite ($CaSO_4$) has been estimated to be 81±7 GPa/155±13 GPa (Yang & Ahrens, 1998). This large difference between gypsum and anhydrite suggests that the stability of sulfur during impact shocks depends on the initial form of the sulfur-bearing sedimentary rocks. As such, the extreme environmental perturbations caused by impact-driven sulfur release during the Cretaceous-Paleogene (K-Pg) impact event (e.g., Ohno et al., 2014) might not have occurred if the bedrock of the impact site was gypsum. Further impact experiments using gypsum and anhydrite, along with solid phase analyses of the solid residues, are necessary to confirm this possibility.

4.3. Implications

Several mechanisms have been proposed that could lead to the lateral transport of Cl-bearing minerals (e.g., Carrier & Kounaves, 2015); that is, transportation by impact ejecta, aqueous films, liquid runoff, or infiltration. We detected vaporization of halite at $P_{1\text{-}D}$ = 18–31 GPa, although the peak I_{58}/I_4 value was only ~1 ppm. Given that these $P_{1\text{-}D}$ values are easily achieved in natural impact events at ~4 km/s (Text S2), impacts onto dry lakebeds at typical impact velocities on Mars would cause shock-induced vaporization of halite. Subsequent expansion of the vapor and condensation of fine NaCl particles would significantly enhance the lateral transport and reactivity of Cl on Mars. Thus, shock-induced vaporization might have been responsible for the production of perchlorates over the Martian surface in the past 3 Gyr, since the hypothesized time of formation of dry lakebeds linked to fluvial activity (e.g., Ramirez & Craddock, 2018). Given the

stochastic nature of natural impacts, the impact-driven transport of Cl from halite lakebeds potentially explains the spatial heterogeneity of Cl on the Martian surface observed by gamma ray spectrometer.

The mass of water vapor M_{H2O} produced from gypsum can be roughly estimated using the method described in Text S3.4. M_{H2O} is at least 0.1–1 times the projectile mass at a $P_{1\text{-}D}$ of 10–110 GPa, even after taking into account the effect of gas escape from the experimental chamber (see Text S3.5). A large volume of anhydrite equivalent to the volume of an impactor might be produced after an impact. Consequently, impact-driven water loss from gypsum could explain the coexistence of gypsum and anhydrite at the Gale crater (e.g., Vaniman et al., 2018), which might have been caused by the events that formed the impact craters found superimposed onto the Gale crater (e.g., Deit et al., 2013). Shocked gypsum ejecta, that is, anhydrite, might have been deposited at/onto the Curiosity sampling sites. In addition, our experiments support the hypothesis that gypsum can serve as a shock indicator, given its high sensitivity at relatively low $P_{1\text{-}D}$ (~10 GPa; e.g., Bell & Zolensky, 2011).

5. Conclusions

We developed a new experimental method to investigate shock-induced vaporization/devolatilization in an open system. This method allows us to use a two-stage light gas gun to investigate the nature of shock-driven phase changes and chemical reactions. Vaporization/devolatilization of evaporitic minerals (halite and gypsum) that are found on Mars were investigated with this method. The shock pressures required for the incipient vaporization of halite and devolatilization of gypsum were estimated to be 18–31 and <11 GPa, respectively. These values are systematically lower than theoretical thermodynamic estimates, suggesting that the initiation of shock-induced gas release is determined by local energy concentrations caused by jetting and shear banding and/or strength-induced irreversible heating. Hypervelocity impacts might have promoted the formation of perchlorates in Martian soil throughout Martian history and be responsible for the coexistence of different forms of Ca-sulfates in the same impact crater.

Acknowledgments
This work was supported by ISAS/JAXA as a collaborative program with its Hypervelocity Impact Facility. We thank Sunao Hasegawa for assistance with the development of our experimental system. We thank Takashi Mikouchi for providing the natural gypsum sample. We appreciate helpful comments by Kojiro Suzuki and Kazuhisa Fujita on the design of the two-valve method. We also thank Reika Yokochi for helpful suggestions about the reduction of background levels of water vapor in our system. We appreciate useful discussions at a workshop on planetary impacts held in 2018 at Kobe University, Japan. The chemical compositions of the rock samples were analyzed by Satoshi Takenouchi at NIMS. We also thank Mattihias Ebert and Christopher Hamann for their constructive reviews that helped greatly improve the manuscript and Andrew J. Dombard for handling the manuscript as an Editor. K. K. is supported by JSPS KAKENHI grants 23840057, 25871212, 17H01176, 17H02990, 17H01175, 17K18812, 18HH04464, and 19H00726 and by the Astrobiology Center of the National Institute of Natural Sciences, NINS (AB261014 and AB281026). Supporting information can be found in the online version of the manuscript. The data supporting the figures are available from the Academic Repository of Chiba Institute of Technology (http://id.nii.ac.jp/1196/00000229/).

References

Ahrens, T. J., & Johnson, M. L. (1995). Shock wave data for minerals. In *Physics and Crystallography* (pp. 28). Washington, DC: American Geophysical Union. https://doi.org/10.1029/RF002p0143

Ahrens, T. J., & O'Keefe, J. D. (1972). Shock melting and vaporization of lunar rocks and materials. *Moon*, *4*(1-2), 214–249. https://doi.org/10.1007/BF00562927

Ballirano, P., & Melis, E. (2009). Thermal behavior and kinetics of dehydration of gypsum in air from in situ real-time laboratory parallel-beam X-ray powder diffraction. *Physics and Chemistry of Minerals*, *36*(7), 391–402. https://doi.org/10.1007/s00269-008-0285-8

Bell, M. S., & Zolensky, M. E. (2011). Experimental shock transformation of gypsum to anhydrite: A new low pressure regime shock indicator, LPS XXXXII, Abstract No. 2008.

Boslough, M. B., Ahrens, T. J., Vizgirda, J., Becker, R. H., & Epstein, S. (1982). Shock-induced devolatilization of calcite. *Earth and Planetary Science Letters*, *61*(1), 166–170. https://doi.org/10.1016/0012-821X(82)90049-8

Brake, D. F., Morris, R. V., Kocurek, G., Morrison, S. M., Downs, R. T., Bish, D., et al. (2013). Curiosity at Gale crater, Mars: Characterization and analysis of the rocknest sand shadow. *Science*, *341*(6153). https://doi.org/10.1126/science.1239505

Carrier, B. L., & Kounaves, S. P. (2015). The origins of perchlorate in the Martian soil. *Geophysical Research Letters*, *42*, 3739–3745. https://doi.org/10.1002/2015GL064290

Clark, B. C., & Kounaves, S. P. (2016). Evidence for the distribution of perchlorates on Mars. *International Journal of Astrobiology*, *15*(4), 311–318. https://doi.org/10.1017/S1473550415000385

Comodi, P., Nazzareni, S., Zanazzi, P. F., & Speziale, S. (2008). High-pressure behavior of gypsum: A single-crystal X-ray study. *American Mineralogist*, *93*(10), 1530–1537. https://doi.org/10.2138/am.2008.2917

Davila, A., Gross, C., Marzo, G. A., Fairén, A. G., Kneissl, T., McKay, C. P., & Dohm, J. M. (2011). A large sedimentary basin in the Terra Sirenum region of the southern highlands of Mars. *Icarus*, *212*(2), 579–589. https://doi.org/10.1016/j.icarus.2010.12.023

Deit, L., Hauber, E., Fueten, F., Pondrelli, M., Rossi, A. P., & Jaumann, R. (2013). Sequence of infilling events in Gale crater, Mars: Results from morphology, stratigraphy, and mineralogy. *Journal of Geophysical Research: Planets*, *118*, 2439–2473. https://doi.org/10.1002/2012JE004322

Ehlmann, B. L., & Edwards, C. S. (2014). Mineralogy of the Martian surface. *Annual Review of Earth and Planetary Sciences*, *42*(1), 291–315. https://doi.org/10.1146/annurev-earth-060313-055024

Fishbaugh, K. E., Poulet, F., Chevrier, V., Langevin, Y., & Bibring, J.-P. (2007). On the origin of gypsum in the Mars north polar region. *Journal of Geophysical Research*, *112*, E07002. https://doi.org/10.1029/2006JE002862

Furukawa, Y., Sekine, T., Oba, M., Kakegawa, T., & Nakazawa, H. (2008). Biomolecule formation by oceanic impacts on early Earth. *Nature Geoscience*, *2*(1), 62–66.

Gordon, S., & McBride, B. J. (1994). Computer program for calculation of complex chemical equilibrium compositions and applications, NASA Reference Publication, 1311.

Hecht, M. H., Kounnaves, S. P., Quinn, R., West, S. J., Young, S. M. M., Ming, D. W., et al. (2009). Detection of perchlorate and the soluble chemistry of Martian soil at the Phoenix lander site. *Science*, *325*(5936), 64–67. https://doi.org/10.1126/science.1172466

Hoerth, T., Schafer, F., Thoma, K., Kenkmann, T., Poelchau, M. H., Lexow, B., & Deutsch, A. (2013). Hypervelocity impacts on dry and wet sand stone: Observations of ejecta dynamics and crater growth. *Meteoritics & Planetary Science*, *48*(1), 23–32. https://doi.org/10.1111/maps.12044

Ishibashi K., Kurosawa, K., Okamoto, T., & Matsui, T. (2017). Generation of reduced carbon compounds by "low" velocity impacts, LPS XLVIII, Abstract No. 2141.

Ishimaru, R., Senshu, H., Sugita, S., & Matsui, T. (2010). A hydrocode calculation coupled with reaction kinetics of carbon compounds within an impact vapor plume and its implications for cometary impacts on Galilean satellites. *Icarus*, *210*(1), 411–423. https://doi.org/10.1016/j.icarus.2010.06.016

Ivanov, B. A., & Deutsch, A. (2002). The phase diagram of $CaCO_3$ in relation to shock compression and decomposition. *Physics of the Earth and Planetary Interiors*, *129*(1-2), 131–143. https://doi.org/10.1016/S0031-9201(01)00268-0

Kawai, N., Tsurui, K., Hasegawa, S., & Sato, E. (2010). Single microparticle launching method using two-stage light gas gun for simulating hypervelocity impacts of micrometeoroids and space debris. *Reviews of Scientific Instruments*, *81*(11), 115105. https://doi.org/10.1063/1.3498896

Keller, J. M., Boynton, W. V., Karunatillake, S., Baker, V. R., Dohm, J. M., Evans, L. G., et al. (2006). Equatorial and midlatitude distribution of chlorine measured by Mars Odyssey GRS. *Journal of Geophysical Research*, *112*, E03S08. https://doi.org/10.1029/2006JE002679

Kieffer, S. W. (1977). Impact conditions required for formation of melt by jetting in silicates. In D. J. Roddy, R. O. Pepin, & R. B. Merrill (Eds.), *Impact and Explosion Cratering* (pp. 751–769). New York: Pergamon Press.

Komatsu, G., Ori, G. G., Marinangeli, L., & Moersch, J. E. (2007). Playa environments on Earth: Possible analogs for Mars. In M. G. Chapman (Ed.), *The geology of Mars: Evidence from Earth-based analogs* (pp. 322–348). Cambridge: Cambridge University Press. https://doi.org/10.1017/CBO9780511536014.014

Kondo, K., & Ahrens, T. J. (1983). Heterogeneous shock-induced thermal radiation in minerals. *Physics and Chemistry of Minerals*, *9*(3-4), 173–181. https://doi.org/10.1007/BF00308375

Kounaves, S. P., Chaniotakis, N. A., Chevrier, V. F., Carrier, B. L., Folds, K. E., Hanses, V. M., et al. (2014). Identification of the perchlorate parent salts at the Phoenix Mars landing site and possible implications. *Icarus*, *232*, 226–231. https://doi.org/10.1016/j.icarus.2014.01.016

Kurosawa, K., & Genda, H. (2018). Effects of friction and plastic deformation in shock-comminuted damaged rocks on impact heating. *Geophysical Research Letters*, *45*, 620–626. https://doi.org/10.1002/2017GL076285

Kurosawa, K., Nagaoka, Y., Senshu, H., Wada, K., Hasegawa, S., Sugita, S., & Matsui, T. (2015). Dynamics of hypervelocity jetting during oblique impacts of spherical projectiles investigated via ultrafast imaging. *Journal Geophysical Research: Planets*, *120*, 1237–1251. https://doi.org/10.1002/2014JE004730

Kurosawa, K., Ohno, S., Sugita, S., Mieno, T., Matsui, T., & Hasegawa, S. (2012). The nature of shock-induced calcite ($CaCO_3$) devolatilization in an open system investigated using a two-stage light gas gun. *Earth Planet Science Letters*, *337–338*, 68–76.

Lodders, K., & Fegley, B. Jr. (1997). An oxygen isotope model for the composition of Mars. *Icarus*, *126*(2), 373–394. https://doi.org/10.1006/icar.1996.5653

Lundborg, N. (1968). Strength of rock-like materials. *International Journal of Rock Mechanics and Mining Sciences*, *5*(5), 427–454. https://doi.org/10.1016/0148-9062(68)90046-6

Marsh, S. P. (1980). *LASL Shock Hugoniot Data*. Berkeley, CA: University of California Press.

Martínez-Pabello, P. U., Navarro-González, R., Walls, X., Pi-Puig, T., González-Chávez, J. L., González-Chávez, J. L., et al. (2019). Production of nitrates and perchlorates by laser ablation of sodium chloride in simulated Martian atmospheres. Implications for their formation by electric discharges in dust devils. *Life Sciences in Space Research*. https://doi.org/10.1016/j.lssr.2019.02.007

Martins, Z., Price, M. C., Goldman, N., Sephton, M. A., & Burchell, M. J. (2013). Shock synthesis of amino acids from impacting cometary and icy planet surface analogues. *Nature Geoscience*, *6*(12), 1045–1049. https://doi.org/10.1038/ngeo1930

McLennan, S. M., Bell, J. F. III, Calvin, W. M., Christensen, P. R., Clark, B. C., de Souza, P. A., et al. (2005). Provenance and diagenesis of the evaporite bearing Burns formation, Meridiani Planum, Mars. *Earth and Planetary Science Letters*, *240*(1), 95–121. https://doi.org/10.1016/j.epsl.2005.09.041

Melosh, H. J. (1989). *Impact cratering: A geologic processes*. New York: Oxford University Press.

Melosh, H. J., & Ivanov, B. A. (2018). Slow impacts on strong targets bring on the heat. *Geophysical Research Letters*, *45*, 2597–2599. https://doi.org/10.1002/2018GL07726

Nakazawa, H., Sekine, T., Kakegawa, T., & Nakazawa, S. (2005). High yield shock synthesis of ammonia from iron, water and nitrogen available on the early Earth. *Earth and Planetary Science Letters*, *235*(1-2), 356–360. https://doi.org/10.1016/j.epsl.2005.03.024

Ohno, S., Kadono, T., Kurosawa, K., Hamura, T., Sakaiya, T., Shigemori, K., et al. (2014). Production of sulphate-rich vapour during the Chicxulub impact and implications for ocean acidification. *Nature geoscience*, *7*(4), 279–282. https://doi.org/10.1038/ngeo2095

Osterloo, M. M., Anderson, F. S., Hamilton, V. E., & Hynek, B. M. (2010). Geologic context of proposed chloride-bearing materials on Mars. *Journal of Geophysical Research*, *115*, E10012. https://doi.org/10.1029/2010JE003613

Osterloo, M. M., Hamilton, V. E., Bandfield, J. L., D, T., Glotch, A. M., Baldridge, P. R., et al. (2008). Chroride-bearing materials in the southern highlands of Mars. *Science*, *319*(5870), 1651–1654. https://doi.org/10.1126/science.1150690

Ramirez, R. M., & Craddock, R. A. (2018). The geological and climatological case for a warmer and wetter early Mars. *Nature geoscience*, *11*(4), 230–237. https://doi.org/10.1038/s41561-018-0093-9

Rao, M. N., Bogard, D. D., Nyquist, L. E., & McKay, D. S. (2002). Neutron capture isotopes in the Martian regolith and implications for Martian atmospheric noble gases. *Icarus*, *156*(2), 352–372. https://doi.org/10.1006/icar.2001.6809

Senshu, H., Kuramoto, K., & Matsui, T. (2002). Thermal evolution of a growing Mars. *Journal of Geophysical Research*, *107*(E12), 5118. https://doi.org/10.1029/2001JE001819

Sugita, S., Kurosawa, K., & Kadono, T. (2012). A semi-analytical on-Hugoniot EOS of condensed matter using a linear Up-Us relation, Shock Compression of Condensed Matter – 2011, AIP Conf. Proc., 1426, 895–898, https://doi.org/10.1063/1.3686412

Trunin, R. F., L. F. Gudarenko, M. V. Zhernokletov, and G. V. Simakov (2001), Experimental data on shock compression and adiabatic expansion of condensed matter, Russ. Federal Nucl. Cent., Sarov, Russia.

Vaniman, D. T., Martinez, G. M., Rampe, E. B., Bristow, T. F., Blake, D. F., Yen, A. S., et al. (2018). Gypsum, basanite, anhydrite at Gale crater, Mars. *American Mineralogist*, *103*(7), 1011–1020. https://doi.org/10.2138/am-2018-6346

Wilson, E. H., Atreya, S. K., Kaiser, R. I., & Mahaffy, P. R. (2016). Perchlorate formation on Mars through surface radiolysis-initiated atmospheric chemistry: A potential mechanism. *Journal of Geophysical Research: Planets*, *121*, 1472–1487. https://doi.org/10.1002/2016JE005078

Wu, Z., Wang, A., Farrell, W. M., Yan, Y., Wang, K., Houghton, J., & Jackson, A. W. (2018). Forming perchlorates on Mars through plasma chemistry during dust events. *Earth and Planetary Science Letters*, *504*, 94–105. https://doi.org/10.1016/j.epsl.2018.08.040

Yang, W., & Ahrens, T. J. (1998). Shock vaporization of anhydrite and global effects on the K/T bolide. *Earth and Planetary Science Letters*, *156*(3-4), 125–140. https://doi.org/10.1016/S0012-821X(98)00006-5

References From the Supporting Information

Bell, M. S. (2016). CO2 release due to impact devolatilization of carbonate: Results of shock experiments. *Meteoritics and Planetary Science*, *51*(4), 619–646. https://doi.org/10.1111/maps.12613

Downs, R. T., & Hall-Wallace, M. (2003). The American Mineralogist Crystal Structure Database. *American Mineralogist*, *88*, 247–250.

Kawaragi, K., Sekine, Y., Kadono, T., Sugita, S., Ohno, S., Ishibashi, K., et al. (2009). Direct measurements of chemical composition of shock-induced gases from calcite: An intense global warming after the Chixulub impact due to the indirect greenhouse effect of carbon monoxide. *Earth and Planetary Science Letters*, *282*(1-4), 56–64. https://doi.org/10.1016/j.epsl.2009.02.037

Lange, M. A., & Ahrens, T. J. (1986). Shock-induced CO_2 loss from $CaCO_3$; Implications for early planetary atmosphere. *Earth and Planetary Science Letters*, *77*(3-4), 409–418. https://doi.org/10.1016/0012-821X(86)90150-0

Martinez, I., Deutsch, A., Schärer, U., Ildefonse, P., Guyot, F., & Agrinier, P. (1995). Shock recovery experiments on dolomite and thermodynamical calculations of impact induced decarbonation. *Journal of Geophysical Research*, *100*(B8), 15,465–15,476. https://doi.org/10.1029/95JB01151

Ohno, S., Kadono, T., Ishibashi, K., Kawaragi, K., Sugita, S., Nakamura, E., & Matsui, T. (2008). Direct measurements of impact devolatilization of calcite using a laser gun. *Geophysical Research Letters*, *35*, L13202. https://doi.org/10.1029/2008GL033796

Pierazzo, E., Kring, D. A., & Melosh, H. J. (1998). Hydrocode simulation of the Chixulub impact event and the production of chemically active gases. *Journal of Geophysical Research*, *103*(E12), 28,607–28,625. https://doi.org/10.1029/98JE02496

Sekine, T., Kobayashi, T., Nishio, M., & Takahashi, E. (2008). Shock equation of state of basalt. *Earth Planets Space*, *60*(9), 999–1003. https://doi.org/10.1186/BF03352857

Vizgirda, J., & Ahrens, T. J. (1982). Shock compression of aragonite and implications for the equation of state of carbonates. *Journal of Geophysical Research*, *87*(B6), 4747–4758. https://doi.org/10.1029/JB087iB06p04747